Lawrence Berkeley National Laboratory
LBL Publications

Title
SOME CONSIDERATIONS ON THE MODELLING OF OXIDE-INDITED FATIGUE CRACK CLOSURE USING SOLUTIONS FOR A RIGID WEDGE INSIDE A LINEAR ELASTIC CRACK

Permalink
https://escholarship.org/uc/item/6g58z8wn

Authors
Suresh, S.
Ritchie, R.O.

Publication Date
1983

Lawrence Berkeley Laboratory
UNIVERSITY OF CALIFORNIA

Materials & Molecular Research Division

SOME CONSIDERATIONS ON THE MODELLING OF OXIDE-INDUCED
FATIGUE CRACK CLOSURE USING SOLUTIONS FOR A RIGID
WEDGE INSIDE A LINEAR ELASTIC CRACK

S. Suresh and R.O. Ritchie

January 1983

DISCLAIMER

SOME CONSIDERATIONS ON THE MODELLING OF
OXIDE-INDUCED FATIGUE CRACK CLOSURE USING
SOLUTIONS FOR A RIGID WEDGE INSIDE A LINEAR ELASTIC CRACK

by

S. Suresh and R. O. Ritchie

Materials and Molecular Research Division, Lawrence Berkeley Laboratory
and Department of Materials Science and Mineral Engineering,
University of California, Berkeley, California   94720

January 1983

SOME CONSIDERATIONS ON THE MODELLING OF OXIDE-INDUCED FATIGUE CRACK CLOSURE USING SOLUTIONS FOR A RIGID WEDGE INSIDE A LINEAR ELASTIC CRACK

S. Suresh and R. O. Ritchie

Materials and Molecular Research Division, Lawrence Berkeley Laboratory and
Department of Materials Science and Mineral Engineering,
University of California, Berkeley, California 94720

Introduction

It has been known for some time that the formation of insoluble corrosion deposits within slowly growing cracks exposed to active environments can produce a mechanical wedging action which can either promote sustained-load cracking (i.e., stress corrosion cracking) (1) or retard cracking under cyclic loads (i.e., corrosion fatigue) (2-6). In the latter case, this wedging action has been shown to be particularly significant for fatigue cracks propagating at near-threshold levels (i.e., typically below 10^{-9} m/cycle) where crack surface oxide debris become comparable in size to the crack tip opening displacements (CTOD) (3-5). In such instances oxide deposits can accumulate near the crack tip to thicknesses some 20 times the naturally-occurring oxide thickness in ambient temperature moist air atmospheres (5) due to a mechanism of "fretting oxidation" (7) from the combined action of plasticity-induced crack closure (8) and Mode II crack tip displacements (9) characteristic of near-threshold crack extension. For example, Auger spectroscopy of near-threshold fatigue fracture surfaces of a bainitic pressure vessel steel (yield strength 500 MPa) tested at 50 Hz at a load ratio $(R = K_{min}/K_{max})$ of 0.05 revealed maximum excess oxide thicknesses close to the threshold stress intensity range (ΔK_0) of 0.2 μm and 0.7 μm in environments of moist air and distilled water, respectively (5,10,11). This is to be compared with a naturally-occurring oxide thickness of 5-15 nm (50-150 Å), measured for metallographically-polished samples exposed to an ambient temperature moist air environment for the same time period. The result of such oxide deposits under cyclic loading is to promote crack tip blunting (12) and more importantly to enhance crack closure through a mechanism which has become known as oxide-induced crack closure (3,5). This effect, however, is most relevant to fatigue cracks growing at near-threshold levels (where CTOD's are small) (5), at low load ratios (where plasticity-induced closure enhances fretting oxidation) (5), in lower strength materials (again to maximize the plasticity-induced closure effect) (3-6,10-13), and of course in environments which promote the formation of corrosion deposits (i.e., in moist oxidizing environments).

Recently, attempts have been made (10,14) to model the role of oxide-induced closure in suppressing rates of environmentally-influenced fatigue crack growth using stress intensity solutions for a rigid wedge inside a linear elastic crack. The purpose of this note is to examine the significance and limitations of this approach in the light of recently available experimental information on near-threshold corrosion fatigue behavior.

The Rigid Wedge Model

As originally proposed by Suresh et al. (10), the significance of oxide films in promoting oxide-induced crack closure where crack tip displacements are small, i.e., at near-threshold levels, can be estimated by considering the simple model of a rigid wedge inside a linear elastic crack. We assume an idealized crack, length a, where the excess oxide layer is taken to be a rigid wedge of constant thickness d, extending along the crack length a distance 2ℓ behind the crack tip (Fig. 1). Assuming only a mechanical closure phenomenon arising from the presence of the oxide wedge and ignoring plasticity, hysteresis and roughness-induced closure (5,15) effects, calculations based on elastic superposition using Barenblatt singular integral

1

equations (16) or the Westergaard stress function (17) yield a resultant stress intensity at the crack tip due to the wedge of (18):

$$K_R \Big|_{x=0} = \frac{E' \, d}{4\sqrt{\pi \ell}} \, , \qquad\qquad (1)$$

where d is the height of the rigid wedge, 2ℓ its location behind the tip and $E' = E$, the elastic modulus, in plane stress and $E' = E/(1 - v^2)$ in plane strain (v = Poisson's ratio). Thus for a fatigue cycle, the crack will close when the stress intensity equals K_R, such that K_R can be taken as the closure stress intensity K_{c1}, and the driving force for crack advance will be reduced from the nominal ΔK (= $K_{max} - K_{min}$) to an effective value ΔK_{eff} (= $K_{max} - K_{c1}$). This can only occur due to oxide formation, however, when the minimum crack tip opening displacement imposed by the fatigue loading cycle is smaller than the excess oxide thickness.

Eq. (1) is evaluated in Fig. 2 for the case of steels, where $E = 2.1 \times 10^5$ MPa and $v = 0.3$, over a range of wedge thickness of 10 nm to 10 μm with ℓ = 10 nm to 100 mm. It is apparent that where significant oxide build-up occurs remote from the crack tip (i.e., for large ℓ), the resultant stress intensity K_R due to the wedge is insignificant for most experimentally observed oxide thicknesses (i.e., d < 1 μm). Conversely for debris formed very close to the tip (i.e., within 0.1 μm) K_R values become extremely large (i.e., $K_R > 5$ MPa$\sqrt{m}$) even for naturally-occurring oxides where d $\simeq$ 15 nm (150 Å). Clearly for this linear elastic model, if oxide forms *at* the tip, $\ell \rightarrow 0$ and the resultant stress intensity becomes infinite.

Factors Affecting the Closure Stress Intensity

The use of Eq. (1) to interpret typical near-threshold fatigue behavior involves 1) determination of the *excess* material (d) inside the crack, 2) consideration of the oxide profile (i.e., thickness as a function of crack length) and in particular where the peak thickness occurs in relation to the crack tip and 3) assessment of the rigidity of the oxide layer.

Typically, crack surface oxide thicknesses have been measured using either Scanning Auger (5,10) or Secondary Ion Mass Spectroscopy (7,19). The uncertainty in such measurements can be up to a factor of two due to the somewhat arbitrary nature of defining the interface between the oxide and the metal (10). To convert such readings into the excess corrosion debris within the crack, calculations involving densities and atomic weights must be made to determine the volume change associated with the oxidation process (10). For steels where the oxide has been identified using ESCA to be predominately Fe_2O_3 (10), one unit volume of Fe oxidizes to roughly 2 unit volumes of oxide (Pilling-Bedworth ratio = 2.13), such that thickness measurements on one half of the fracture surface represent approximately the total excess material (d), assuming only thickness-direction growth and equal thicknesses on each crack face. For aluminum alloys where the Pilling-Bedworth ratio is 1.3, the total excess Al_2O_3 thickness is about one half of the value measured by ion sputtering (19).

Estimation of the oxide profile and the value of ℓ, however, is more complex since in many instances the crack surface oxide wedge is not of constant thickness. In situations where the oxidation occurs naturally and does not primarily evolve from a fretting process, such as at high load ratios (5), in very oxidizing environments (11) (e.g., water), in high strength steels (13,20), and in 2000 series and peak-aged 7000 series aluminum alloys (19), oxide films are fairly uniform (Fig. 3b,c). However, for lower strength steels (5), copper (21) and (overaged) 7075-T7 aluminum alloys (19) tested at low load ratios, where the accumulation of crack surface oxide occurs primarily by fretting oxidation (5,11), the oxide thickness measured at a particular crack length at the completion of the test is found to be inversely related to the crack growth rate corresponding to that crack length (5). The oxide thickness profile thus depends upon the previous cyclic load history and can be very non-uniform. For decreasing stress intensity (load shedding) sequences conventionally applied in near-threshold testing, the oxide thickness tends to increase with crack length up to a peak value (d_0) close to where the threshold was measured, as shown for the data for 7075-T7 in Fig. 3a. Idealizing such a profile as a wedge of constant thickness does not appear very feasible, but attempts to employ more rigorous calculations using a realistic variable thickness wedge proved unsuccessful because of uncertainties in the location of the peak thickness behind the tip, with the exact nature of contact between the faces and with the oxide profile from the peak to the crack tip (10). However, since the profiles experimentally observed both for lower strength steels (5,10) and 7075-T7 (19) are heavily "spiked" at the peak value (close to ΔK_0), and since the debris

behind this peak (i.e., more remote from the tip) will, from Eq. (1), have a much smaller influence on the wedge force (i.e., K_R), it appears reasonable to take the wedge thickness to be the peak oxide thickness ($d = d_0$) in attempting to model the extent of closure at the threshold ΔK_0 value (10). Determination of the location of this peak behind the crack tip at ΔK_0 (i.e., 2ℓ) is even more complex because this dimension is often too small to resolve experimentally. Scanning electron microscopy of near-threshold fracture surfaces in 2¼Cr-1Mo steel (SA542-3), where cracks were grown in moist air at R = 0.05 via a load-shedding procedure to ΔK_0 and then broken open in liquid nitrogen, did, however, indicate the oxide peak to be within 1 to 5 μm of the crack tip (10,11). Further definition of the value of ℓ or the nature of the oxide profile in this immediate vicinity of the tip was not possible. Since K_R, from Fig. 2, depends critically on the value of ℓ (albeit to a square root dependence), the experimental uncertainty in this value poses a severe limitation in the predictive capacity of this model.

Finally, the model assumes the oxide layer to have sufficient compressive strength to remain essentially rigid to support the wedge load. Although mechanical property data for relevant oxides in the constrained condition within a crack are not available, estimates by Hudak and Page (14) indicate the compressive strength of iron oxides to be between 1400 and 2500 MPa. Since this is a factor of 3 to 5 times harder than the lower strength steels where oxide-induced closure has been shown to be a major influence on near-threshold behavior (5), assumptions of a rigid oxide wedge would appear to be feasible.

Application to Near-Threshold Fatigue Behavior

In general, corrosion fatigue crack growth behavior, particularly at near-threshold levels, must be considered in terms of two mutually competitive mechanisms, namely active-path corrosion (metal dissolution) and/or hydrogen embrittlement (due to the release of cathodic hydrogen) from the crack tip oxidation process which *increase* growth rates, and crack closure mechanisms from the resultant oxidation products (or additionally wedging from rough fracture morphologies (15)) which *decrease* growth rates. Accordingly, care must be taken in interpreting environmentally-influenced near-threshold behavior solely in terms of the oxide wedge model outlined above since more often than one mechanism is at play. However, lower strength steels (yield strengths ∿ 500 MPa) tested at the frequencies generally employed for near-threshold tests (i.e., > 25 Hz) provide an ideal test case since at these frequencies contributions at ultralow growth rates to crack advance from hydrogen embrittlement and active path corrosion mechanisms are generally minimal. Accordingly, compared to behavior in room air at low load ratios, the marginally slower near-threshold growth rates in moist environments (i.e., water and wet hydrogen gas) and the faster growth rates in dry environments (i.e., dehumidified helium or hydrogen gas) have been interpreted in terms of the extent of crack surface oxidation debris and hence oxide-induced closure (5). Relevant threshold data, taken from refs. 5, 10 and 11 for a bainitic 2¼Cr-1Mo steel, are listed in Table 1.

Thus, considering first the threshold in moist air at R = 0.05 ($\Delta K_0 = 7.7$ MPa√m) where the maximum oxide thickness was measured as $d_0 \simeq 0.2$ μm, taking $\ell \sim 2$ μm (from scanning electron micrographs) yields an estimate of the closure stress intensity ($K_{c\ell} = K_R$) from Eq. (1) of ∿ 4.7 MPa√m. For R = 0.05 tests in dry hydrogen ($\Delta K_0 = 5.2$ MPa√m) where $d_0 \simeq 0.1$ μm, $K_{c\ell}$ is estimated to be 2.1 MPa√m. Thus the predicted difference in closure stress intensities for moist air and dry hydrogen at threshold due to the presence of oxide debris is of the order of 2.5 MPa√m, approximately equal to the difference in the observed ΔK_0 values for the two environments. Calculations for the closure stress intensities at R = 0.75 in either environments, where only the naturally-occurring limiting oxide thickness is seen (i.e., $d_0 \sim 5$-15 nm), yield negligible $K_{c\ell}$ values between 0.1 and 0.3 MPa√m, consistent with the fact that closure effects are minimal at high load ratios. These $K_{c\ell}$ values, predicted from Eq. (1), compare reasonably well with experimental measurements of closure stress intensities in this steel at threshold, determined using an ultrasonic technique (10,11), as shown in Table 1.

Thus, despite the crude nature of the model, uncertainties in the measured values and the assumption that the levels of plasticity-induced and roughness-induced closure are identical in the above set of data, it is clear that this wedge model can give an appreciation of how oxide-induced closure influences near-threshold crack growth. However, for *quantitative* prediction, the model is extremely limited since the value of ℓ, the distance of the peak oxide thickness behind the crack tip, must be used essentially as a fitting parameter. This follows from the difficulties in experimental measurement of ℓ, and more importantly because mechanisms of crack surface fretting oxidation and hence the factors that physically govern ℓ are simply

not understood. Oxide clearly forms thermally directly on the material freshly exposed at the crack tip. However, for such oxide to build up to the thicknesses measured (i.e., up to 20 times the natural limiting thickness), it must be broken up through the physical contact between crack surfaces (from crack closure) and from the presence of Mode II crack tip displacements, and then deposited into the crack until it accumulates to a peak level where, at the threshold, it can lead to crack arrest. It is not possible to predict, however, where this peak level is in relation to the tip. This can be appreciated by examining threshold data in Table 1 for a more oxidizing medium such as distilled water. At $R = 0.05$, the threshold in water is essentially identical to the threshold in moist air, yet the extent of crack surface oxidation is much greater (i.e., d_0 is over three times larger in water). For the closure stress intensities and hence ΔK_0 values to be similar in these two environments, Eq. (1) demands ℓ to be 7 μm in water whereas experimental measurements suggest ℓ to be ~ 2 μm in moist air. Since in water environments it is inevitable that oxidation will continue during and subsequent to the point of threshold measurement, one cannot be certain whether such differences in the value of ℓ between moist air and water are physically sensible or simply that the oxide measurements performed at the completion of the test do not truely reflect the oxide thicknesses at the initial point of crack arrest. Thus, in view of these uncertainties, and the assumptions outlined above, we conclude that *a priori* predictions or more rigorous calculations of K_{cl} with this model are simply not warranted.

Finally, in this regard, Hudak and Page use Eq. (1) to compute closure stress intensities for service cracks in steam turbine discs of 3Cr-1Mo and 3.5Ni-Cr-Mo-V steels (14). Using oxide thickness measurements (d) *very* remote of the crack tip at $\ell/a \sim 0.9$ (where neither values of d, ℓ and a are stated but crack lengths appear to be of the order of a $\sim$ 60mm), they predict K_R values to be between 8 and 17 MPa$\sqrt{m}$. They further state that the distribution of oxides on the crack surfaces was very different to that described above for near-threshold laboratory tests (e.g., Fig. 3). However, since the *near-tip* oxide distribution was not analyzed and since this will clearly *dominate* in the development of a wedge stress intensity K_R, as clearly shown in Fig. 2 (e.g., 150 Å of oxide at 20 nm from the crack tip has a larger effect on K_R than 10 μm of oxide at 20 mm from the tip!), the validity of their closure estimates are somewhat questionable.

Conclusions

The significance and limitations of the simple model of a rigid wedge inside a linear elastic crack, used to estimate closure stress intensities resulting from the formation of corrosion deposits during corrosion fatigue, are described. The resultant closure stress intensities predicted by the model are shown to be a strong function of the wedge thickness and its location directly behind the crack tip. Although the wedge thickness can be experimentally estimated by computing the excess oxide thickness from Auger and Secondary Ion Mass Spectroscopy measurements, the oxide film profile in the *immediate* vicinity of the crack tip is difficult to resolve. Since this near-tip oxide distribution is critical in the estimation of the wedge force, more rigorous calculations of the extent of oxide-induced crack closure are not feasible.

Acknowledgements

References

1. H. W. Pickering, F. H. Beck and M. G. Fontana: Corrosion, 18, 230 (1962).
2. K. Endo, K. Komai and Y. Matsuda: Memo Fac. Eng., Kyoto Univ., 31, 25 (1969).
3. R. O. Ritchie, S. Suresh and C. M. Moss: J. Eng. Matls. Tech., Trans. ASME Ser. H, 102, 293 (1980).
4. A. T. Stewart: Eng. Fract. Mech., 13, 463 (1980).
5. S. Suresh, G. F. Zamiski and R. O. Ritchie: Met. Trans. A, 12A, 1435 (1981).
6. H. Kitagawa, S. Toyohira and K. Ikeda: in Fracture Mechanics in Eng. Appl., G. C. Sih and S. R. Valluri, eds., Sijthoff & Noordhoff (1981).
7. D. Benoit, R. Namdar-Irani and R. Tixier: Mater. Sci. Eng., 45, 1 (1981).
8. W. Elber: ASTM Spec. Tech. Publ. 486, p. 280 (1971).
9. D. L. Davidson: Fat. Eng. Mat. Struct., 3, 229 (1981).
10. S. Suresh, D. M. Parks and R. O. Ritchie: in Fatigue Thresholds, J. Bäcklund, A. Blom and C. J. Beevers, eds., EMAS Ltd., vol. 1, p. 391 (1982).

11. S. Suresh and R. O. Ritchie: Eng. Fract. Mech., 17 (1983), in press.
12. F. P. Ford: in BWR Environmental Cracking Margins for Carbon Steel Piping, Final Report RP 1248/1, Electric Power Research Institute, Palo Alto (1981).
13. R. O. Ritchie, S. Suresh and P. K. Liaw: in Ultrasonic Fatigue, J. M. Wells, O. Buck, L. D. Roth and J. K. Tien, eds., TMS-AIME, p. 443 (1982).
14. S. J. Hudak and R. A. Page: Corrosion, 29 (1983), in press.
15. S. Suresh and R. O. Ritchie: Met. Trans. A, 13A, 1627 (1982).
16. G. L. Barenblatt: in Advances in Applied Mathematics, Academic Press, vol. 7, p. 55 (1962).
17. H. M. Westergaard: J. Appl. Mech., Trans. ASME Ser. A, 66, 49 (1939).
18. H. Tada, P. C. Paris and G. R. Irwin: in Stress Analysis of Cracks Handbook, Del Research Corp. (1976).
19. A. K. Vasudévan and S. Suresh: Met. Trans. A, 13A, 2271 (1982).
20. J. Toplosky and R. O. Ritchie: Scripta Met., 15, 905 (1981).
21. P. K. Liaw, T. R. Leax, R. S. Williams and M. G. Peck: Met. Trans. A, 13A, 1607 (1982).

TABLE 1

Comparison of Predicted (From Eq. (1)) and Measured Closure Stress Intensities (K_{cl}) for Bainitic 2¼Cr-1Mo Steel at Threshold

| Environment	Load Ratio (R)	Max. Excess Oxide Thickness (d_o)	ΔK_o	K_{cl} (measured)	K_{cl} (predicted)
	(K_{min}/K_{max})	(μm)	(MPa$\sqrt{m}$)	(MPa$\sqrt{m}$)	(MPa$\sqrt{m}$)
moist air	0.05	0.20	7.7	4	4.7
dry hydrogen	0.05	0.09	5.2	2	2.1
water	0.05	0.70	7.8	-	4.8
moist air	0.75	0.01	3.2	< 1	0.2
dry hydrogen	0.75	0.01	3.3	-	0.2

Oxide wedge

y

x

d

2ℓ

a
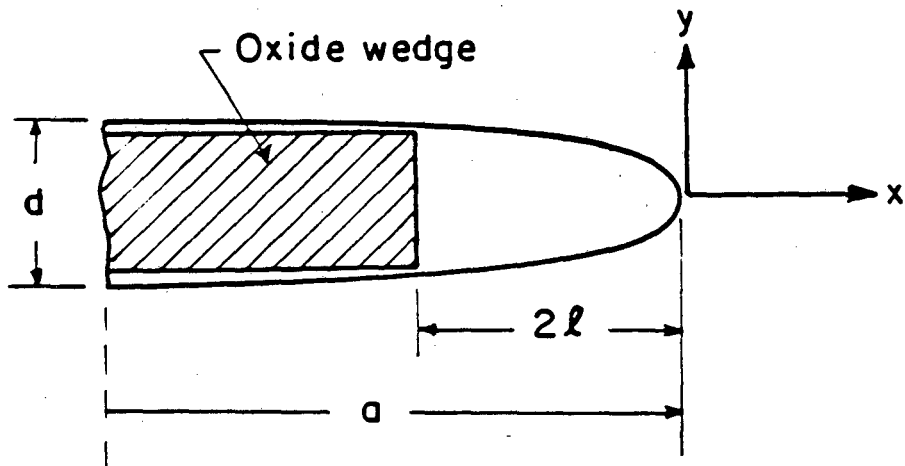
XBL 832-5178

FIG. 1. Idealization of the role of crack face oxide debris in influencing near-threshold fatigue crack extension in terms of a rigid wedge within a linear elastic crack.

6
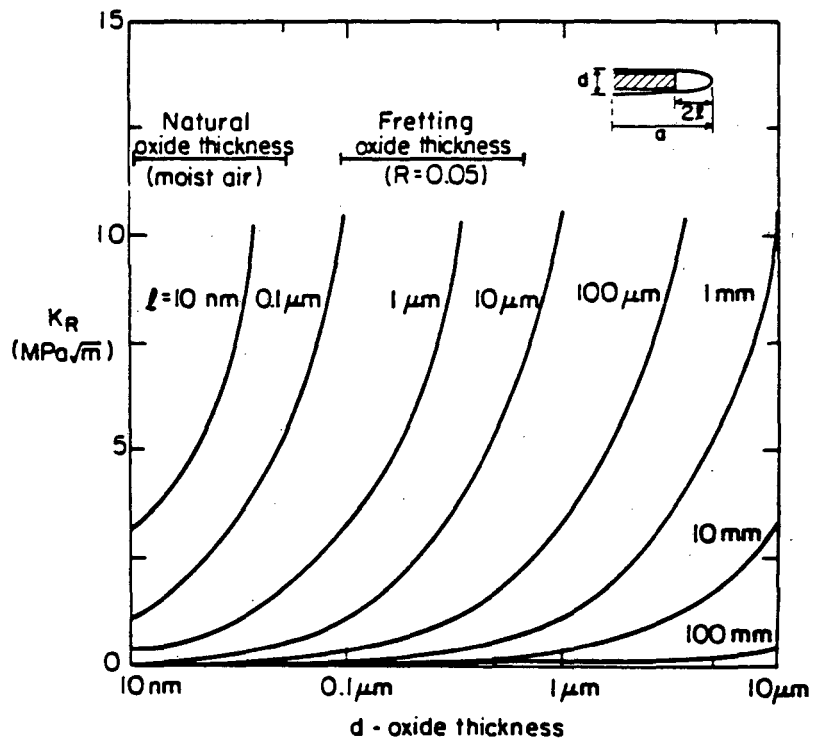
FIG. 2. Computation of the value of the resultant stress intensity K_R due to a rigid wedge of constant thickness (d) located distance 2ℓ behind the crack tip (Eq. (1)). Calculations for steel where the elastic modulus $E = 2.1 \times 10^5$ MPa and Poisson's ratio $\nu = 0.3$.

7
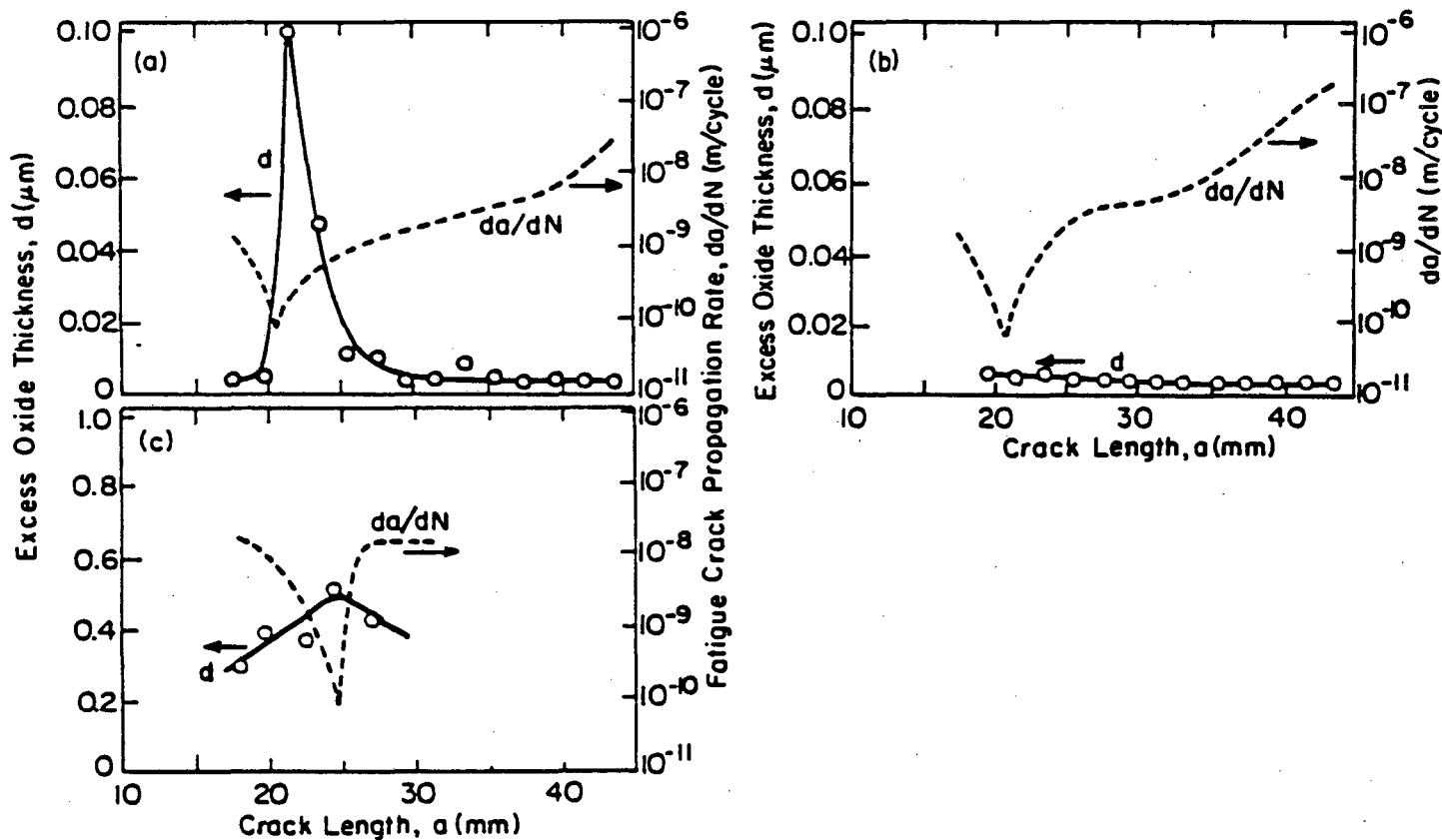
FIG. 3. Variation of the thickness (d) of crack face oxidation products as a function of crack length (a) and crack growth rate (da/dN) for a) 7075-T7 overaged and b) 7075-T6 peak aged aluminum alloys tested at R = 0.33 in 95% relative humidity moist air, and c) SA542-3 2¼Cr-1Mo steel tested at R = 0.05 in distilled water. Date from refs. 11 and 19.